J Incl Phenom Macrocycl Chem (2011) 69:403–409
DOI 10.1007/s10847-010-9772-x

ORIGINAL ARTICLE

HR MAS NMR, powder XRD and Raman spectroscopy study of inclusion phenomena in βCD nanosponges

Andrea Mele · Franca Castiglione · Luciana Malpezzi · Fabio Ganazzoli · Giuseppina Raffaini · Francesco Trotta · Barbara Rossi · Aldo Fontana · Giovanni Giunchi

Received: 20 November 2009 / Accepted: 16 March 2010 / Published online: 30 March 2010

Abstract Three different samples of β cyclodextrin nanosponges (CDNS) are prepared from β cyclodextrin (βCD) and pyromellitic dianhydride (PMA). CDNS are cross-linked, nanoporous materials whose pore size can be modulated by suitable choice of the CD/PMA molar ratio. In the presence of aqueous solutions they can swell giving rise to gel-like behavior. The Raman spectra of dry and water treated CDNS are described, with emphasis on the group vibration modes in the low frequency part of spectrum, sensitive to molecular environment and cross-linking degree, and on O–H/C–H vibration modes of dry/swollen CDNS, in turn providing information on the hydration dynamics. Powder X-ray diffraction data indicate low crystallinity and the presence of bulk water within the 3D polymer network. High resolution magic angle spinning (HR MAS) NMR spectroscopy is successfully used for investigation of swollen CDNS. The NMR signals of bulk and "bound" water indicate two different states of water molecules inside the gel. Probe solute fluorescein is used to spot on the diffusion properties inside the gel. In one case the diffusion coefficient of fluorescein measured in CDNS results one order of magnitude higher than that in D_2O. The acceleration effect uncovered indicates that the motion of fluorescein inside the porous gel is driven by both hydrodynamic and electrostatic factors.

Keywords Cyclodextrin nanosponges · HR MAS NMR · Raman · X-ray diffraction · Diffusion

Introduction

Cyclodextrin nanosponges (CDNS) belong to an important class of polymers obtained by reacting a suitable CD–βCD in the present work–with cross-linking agents, diisocyanates, carboxylic acids dianhydrides or activated carbonyl compounds [1–5]. The final products are cross-linked polymers with intriguing properties of swelling, absorption/inclusion of chemicals, and release of active compounds. Thus, several applications have been proposed, especially in the fields of controlled release of pharmaceutical active ingredients [6–8] and environmental chemistry [9–12]. Despite the continuously growing repertoire of possible uses of CDNS, a thorough characterization in terms of molecular structure is still missing. This is largely due to the intrinsic difficulty of investigation of these systems at the molecular level, in turn connected to the random nature of the growing process of the polymer. Moreover, the different cross-linking agents may dramatically modulate important parameters such as the swelling capability and hydrophilicity/hydrophobicity of the final polymer. With this picture in mind, a long-term project was started with the main goal of a deep understanding of the molecular environment within the 3D network of the

A. Mele (✉) · F. Castiglione · L. Malpezzi · F. Ganazzoli · G. Raffaini
Dipartimento di Chimica, Materiali e Ingegneria Chimica "G. Natta", Politecnico di Milano, Via L. Mancinelli 7, 20131 Milano, Italy
e-mail: andrea.mele@polimi.it

F. Trotta
Dipartimento di Chimica IFM, Università di Torino, Via Pietro Giuria 7, 10125 Torino, Italy

B. Rossi · A. Fontana
Dipartimento di Fisica, Università di Trento, Via Sommarive 14, 38123 Povo (TN), Italy

G. Giunchi
EDISON SpA-R&D Division, Foro Buonaparte 31, 20121 Milano, Italy

CDNS. To this end, different physical methods of investigation are being used. In the present paper we present some preliminary results on CDNS obtained from βCD and pyromellitic dianhydride PMA (see Fig. 1) at three different βCD/PMA molar ratios. The latter parameter is expected to affect the degree of cross-linking of the polymer and, in turn, the swelling ability of the material. Our attention was mainly focused on two different aspects: i) to explore the possibility of using powerful solid-state structural methods like Raman spectroscopy and X-ray crystallography to describe the behavior of the CDNS on passing from the dry to the swollen state; ii) to gain information on the state of water and a model solute dissolved in water inside the nanoporous network of swollen CDNS, with particular emphasis on the diffusion phenomena in the gel-like state.

Experimental

Synthesis of CDNS

The nanosponges were obtained following the synthetic procedure reported in the Italian patent with minor modification [13]. The molecular ratios of reagents were 1:2, 1:4 and 1:8 for β cyclodextrin and pyromellitic dianhydride, respectively (see Fig. 1 for the adopted nomenclature).

The reagents, dissolved in DMSO containing triethylamine were allowed to react at room temperature for 3 h. Once the reaction was over the solid obtained was ground in a mortar and Soxhlet extracted with acetone for 8 h.

Raman spectroscopy

Raman spectra of βCDNS were recorded at room temperature by means of a microprobe setup (Horiba-Jobin-Yvon, LabRam Aramis) consisting of a He–Ne laser, a narrow-band notch filter, a 46 cm focal length spectrograph using a 1800 grooves/mm grating and a charge-coupled device (CCD) detector. Exciting radiation at 632.8 nm was focused onto the sample surface with a spot size of about 1 μm^2 through a 100× objective with NA = 0.9. To avoid unwanted laser-induced transformations, neutral filters of different optical densities were used, whenever necessary. Spectra were collected in the wavenumber ranges 100–3700 cm^{-1}. The resolution was about 0.35 cm^{-1}/pixel.

For the Raman spectra acquired in the wavenumber range between 5 and 100 cm^{-1}, a triple-monochromator spectrometer (Horiba-Jobin-Yvon, model T64000) set in double-subtractive/single configuration and equipped with 1800 grooves/mm grating was used. Micro-Raman spectra were excited by the 514.5 nm wavelength of an argon/krypton ion laser and detected by a CCD detector. The resolution was about 0.6 cm^{-1}/pixel.

Raman scattering observed from all the samples was generally superimposed over a continuous, nearly flat luminescence background, which was properly accounted for in the spectra analysis by comparing replicated spectra of each sample over the whole spectral range.

X-ray crystallography

The X-ray powder diffraction (XRPD) patterns of the powdered samples were collected at room temperature on an Ital-Structure θ/θ automated diffractometer, under the following conditions: Ni-filtered, CuKα ($\lambda = 1.5418$ Å) radiation; diffraction angles range $3 \leq 2\theta \leq 40°$; step width 0.04°cm; step counting time 1 s; voltage 40 kV, current 30 mA.

NMR spectroscopy

The ^1H NMR spectra were recorded on a Bruker Avance spectrometer operating at 500 MHz proton frequency equipped with a dual $^1H/^{13}C$ HR MAS (high resolution magic angle spinning) probe head for semi-solid samples. Samples were transferred in a 4 mm ZrO_2 rotor containing a volume of about 50 μL. All the ^1H spectra were acquired with a spinning rate of 4 kHz to eliminate the dipolar contribution. Self-diffusion coefficients were measured by diffusion ordered correlation spectroscopy (DOSY) experiments. A pulsed gradient unit capable of producing

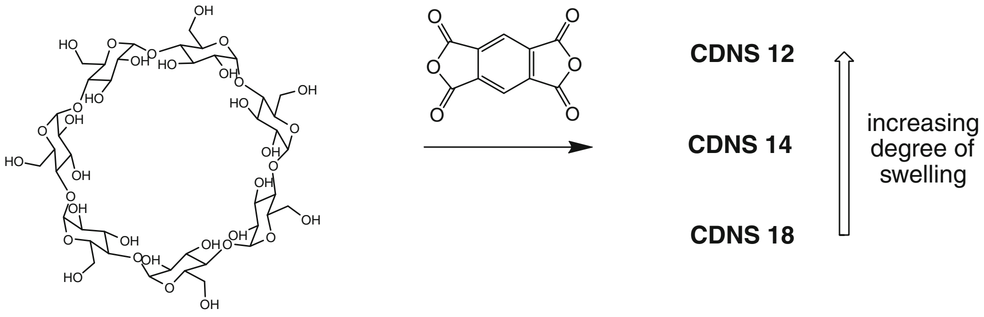

Fig. 1 Scheme of the synthesis of CDNS. The *numbers* refer to the molar ratio between reagents (e.g. CDNS12 = polymer obtained from βCD and PMA in molar ratio 1:2, respectively)

magnetic field pulse gradients in the z-direction of 53 G cm^{-1} was used. These experiments were performed using the bipolar pulse longitudinal eddy current delay (BPLED) pulse sequence. The duration of the magnetic field pulse gradients (δ) and the diffusion times (Δ) was optimized for each sample in order to obtain complete dephasing of the signals with the maximum gradient strength. In each DOSY experiment, a series of 64 spectra with 32 K points were collected. For each experiment 16 scans were acquired. For the investigated samples, Δ was set to 0.1 s, while the δ values were in the range 0.5–2.5 ms. The pulse gradients were incremented from 2 to 95% of the maximum gradient strength in a linear ramp. The temperature was set and controlled at 300 K with an air flow of 535 L h^{-1} in order to avoid any temperature fluctuations due to sample heating during the magnetic field pulse gradients.

Sample preparation

Two different types of samples were prepared for HR MAS NMR experiments: CDNS swollen with D_2O and CDNS swollen with fluorescein solutions (100 mg/mL) in D_2O. The samples were prepared in order to get—as a first approximation—comparable swelling ratios r for all the samples. The swelling ratio was determined as $r =$ m(swollen)/m(dry) [14]. In a typical procedure for the preparation of samples of D_2O swollen CDNS, 50 mg of CDNS12 or CDNS14 were allowed to swell for 3–4 days with 300 μL of D_2O, affording gels with $r = 7$. Lower r (not determined) was obtained in the case of CDNS18. The same protocol was followed for the preparation of CDNS swollen with fluorescein solution. The final aspect of the swollen nanosponges ranged from gel-like (CDNS12, CDNS14) to solid-like (CDNS18).

Results and discussion

Raman spectroscopy

The Raman spectroscopy is a useful tool for studying molecular structures because the width and the intensity, as well as the wavenumber of the Raman peaks, are sensitive to the environmental and conformational changes of the molecules and to the intermolecular interactions. In this paper only two aspects will be discussed: the analysis of the low-frequency region of the spectrum and the comparison of the hydration process of CDNS as monitored by Raman scattering.

Figure 2 displays a zoom the Raman spectra of the investigated CDNS in the low wavenumbers region. A characteristic bump, well known in disordered systems [15, 16], centered at about 15–30 cm^{-1} is clearly visible. This is likely to be related to the collective vibration modes of the system, while a quasielastic scattering contribution for wavenumber lower than 5 cm^{-1} appears as a broadened elastic line. Also, in this wavenumber range the spectra of the three investigated CDNS exhibit different spectral profiles, thus suggesting changes in the low-energy vibrational dynamics connected to the increasing density of cross-linking of the whole system. Moreover, in the spectra of CDNS18, a broad band at about 90 cm^{-1}, not detectable in the spectra of CDNS14 and 12, can be observed. However, the analysis of these data is still preliminary and it requires further measurements at low temperatures in order to decrease the strong elastic and quasielastic contribution which is superimposed to the spectral components directly related to the vibrational dynamics.

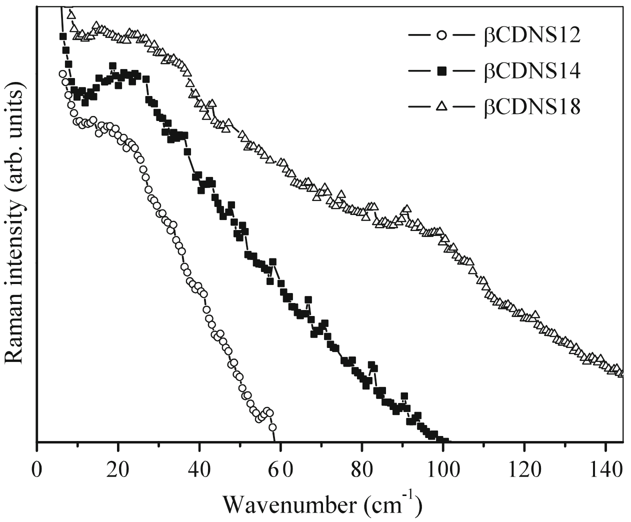

Fig. 2 VV Raman spectra of dry CDNS12 (*empty circle*), CDNS14 (*black squares*) and CDNS18 (*empty triangles*) in the low-wavenumber range between 5 and 150 cm^{-1}

Under the assumption that changes in the spectral features observed in the Raman spectra of CDNS can be associated with structural changes in the polymer network [17], the hydration process of CDNS14 was analyzed. In Fig. 3 we compare the Raman spectra recorded on dry (a) and water-treated (b) sample of CDNS14, in the energy region between 2800 and 3150, where the most significant changes in the CDNS spectra as a consequence of hydration can be observed. The analysis of the changes detected in the spectra in the frequency range 200–3100 cm^{-1} will be not here discussed. For a finer investigation, the spectral contribution of the intramolecular O–H stretching vibration of bulk water (3000–3800 cm^{-1}) which is partially superimposed to the modes of CDNS were modeled with fives modes fitted by using Gaussian functions as in [17] and previously subtracted from the total signal of Fig. 3b. In this way, the hydration-induced changes of the O–H and

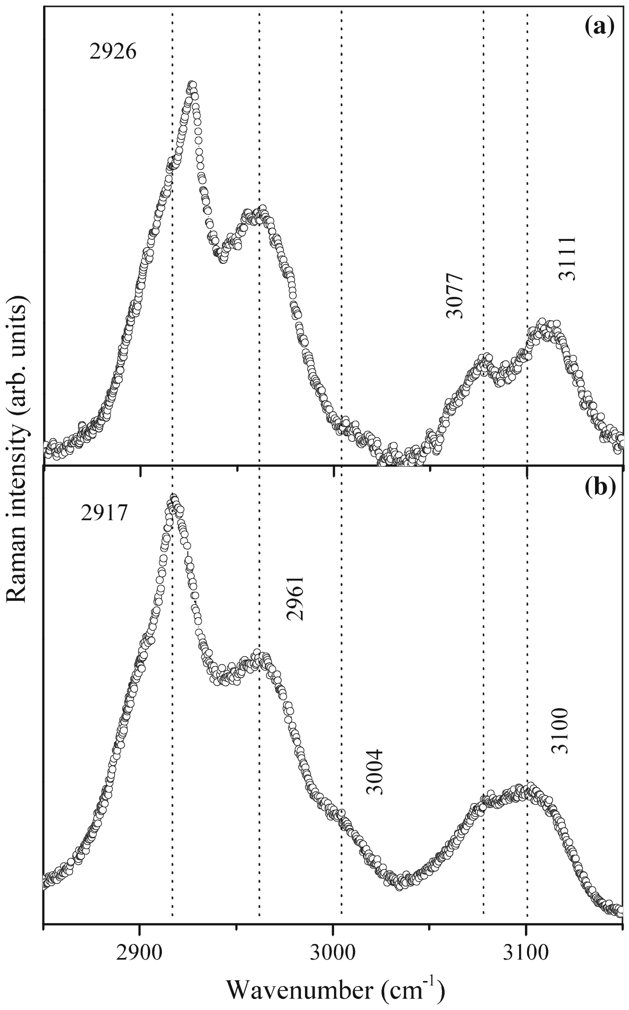

Fig. 3 VV Raman spectra of CDNS14 dry (**a**), and treated with water (**b**) in the wavenumber range 2800–3150 cm^{-1}. *Dashed lines* indicate the wavenumber of main peaks

C–H vibration modes in the CDNS spectrum could be readily observed. As it is evident in Fig. 3, the intensity ratio between the broad bands around 3100 cm^{-1} (which shift to 3111 cm^{-1} in hydrated CDNS) and 3077 cm^{-1} significantly changes with hydration, suggesting that the hydration process affects these vibration modes. The band which falls at 2961 cm^{-1} in dry sample of CDNS does not seem show frequency or intensity changes with hydration, while we observe a significant decreasing in intensity of the bump at 3004 cm^{-1} with hydration.

In addition, we observe an interesting change of the mode centered at 2917 cm^{-1} in dry CDNS which shifts to higher wavenumber (2926 cm^{-1}) in water-treated sample spectrum, suggesting a hardening of the bond involved in this vibration mode. These changes, readily monitored by Raman intensity and frequency, suggest structural changes in the polymer network of CDNS14 as a consequence of hydration process.

X-ray diffraction

Powder XRD spectra of the three CDNS are reported in Fig. 4. All the examined CDNS are predominantly amorphous, as clearly shown by the typical diffracting haloes in the XRD powder patterns. The diffraction distance d, corresponding to the maximum of the haloes according to the Bragg equation, is correlated with the statistically most recurring nonbonded inter-atoms distance in the compound, so a shift of the maximum means a change in the molecular contacts at the atomic level. This distance for all the dry CDNS samples is around 4.6 Å. Only CDNS18 presents several crystalline peaks, indicating that a different spacer position between the CD moieties can favor their crystallinity.

The samples CDNS14 and CDNS12, when treated with water, swell to larger volumes, absorbing a large quantity of water. As shown in Fig. 4, the maximum of the diffracting halo of the water swollen samples shifts to lower d-spacings (higher 2θ) with respect to the corresponding pure samples. We interpret this behavior as due to the dominant scattering of the water molecules in the water treated samples. Indeed the X-ray diffraction patterns of the swollen CDNS are very similar to that of the pure water, with the maximum of the halo at a d value of about 3.12–3.25 Å ($\mathrm{dH_2O} = 3.12$ Å). These results confirm the existence of free water inside the polymeric network. Further aspects of the state of water inside the swollen nanosponges are provided by NMR (see next section).

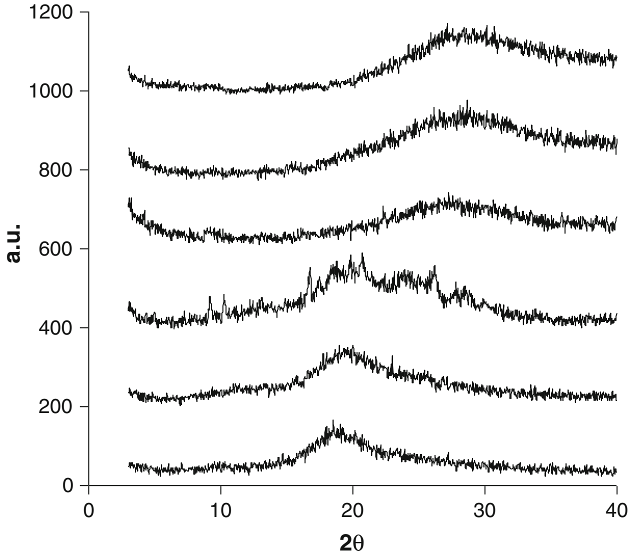

Fig. 4 XRD patterns of CDNS. From *bottom to top*: CDNS12 (dry powder), CDNS14 (dry powder), CDNS18 (dry powder), CDNS12 (swollen with water), CDNS14 (swollen with water), water (pure liquid, reference)

HR MAS NMR

High resolution magic angle spinning (HR MAS) NMR is a powerful technique able to provide high resolution NMR spectra from semi-solid or heterogeneous samples. Line broadening due to dipolar relaxation and susceptibility distortions are dramatically reduced by orienting the sample at the magic angle (54.7°) with respect to static B_0 field and spinning the sample at suitable rate (spinning rate 2–10 kHz generally). Liquid-like NMR spectra can be obtained from large aggregates [18], organic ligands supported on polymers [19, 20], and ex-vivo samples [21]. In the present study, medium to high resolution NMR spectra could be obtained for CDNS12 and CDNS14 swollen with a D_2O solution of fluorescein, as reported in Fig. 5. The analysis of the spectra provides two important indications: (i) the fluorescein spectrum is well resolved (especially in CDNS14), showing that fluorescein exists inside the gel as free, non-aggregated molecules; (ii) there are two different signals assignable to residual water (HOD). Further information on the state of solute and solvent within the 3D structure of the cross-linked CDNS were obtained by measuring the self diffusion constants D of both components in the two nanosponges. The results are summarized in Table 1. The data on diffusivity point out the presence of two different types of water molecules in the swollen CDNS: "free" (or bulk) and "bound" water. The measured self-diffusion coefficient of the former satisfactorily matches the literature reference value [22], with small variations likely due to different amounts of deuterium exchange, small temperature variations due to spinning, etc. The D values measured for the other type of water ("bound") are indeed one order of magnitude lower, indicating a decreased mobility. At this stage, only tentative explanations can be proposed, such as water molecules entrapped in polar clefts within the cross-linked polymer, hydrogen bound to CD free hydroxyl groups or included into the CD cavities as relatively isolated clusters [23]. It is worth noting, however, that the presence of two different states of water, detectable as individual signals in slow exchange on the NMR time-scale, is an intriguing feature of CDNS and indicates the presence of two different molecular environments: large pores where the solvent shows bulk behavior, and either polar sites of binding where water molecules are tightly attached, or the CD cavities with small clusters of molecules.

Table 1 Self-diffusion coefficients (m^2/s) measured by HR MAS NMR

System	D (water "free")	D (water bound)	D (fluorescein)
CDNS12	1.6×10^{-9}	1.7×10^{-10}	3.2×10^{-10}
CDNS14	2.6×10^{-9}	6.5×10^{-10}	3.8×10^{-9}
Reference[a]	2.299×10^{-9}		3.2×10^{-10}

[a] For water: see Ref. [22]. For fluorescein: the reference value was measured (this work) for a D_2O solution of the same concentration (100 mg/mL) at the same temperature

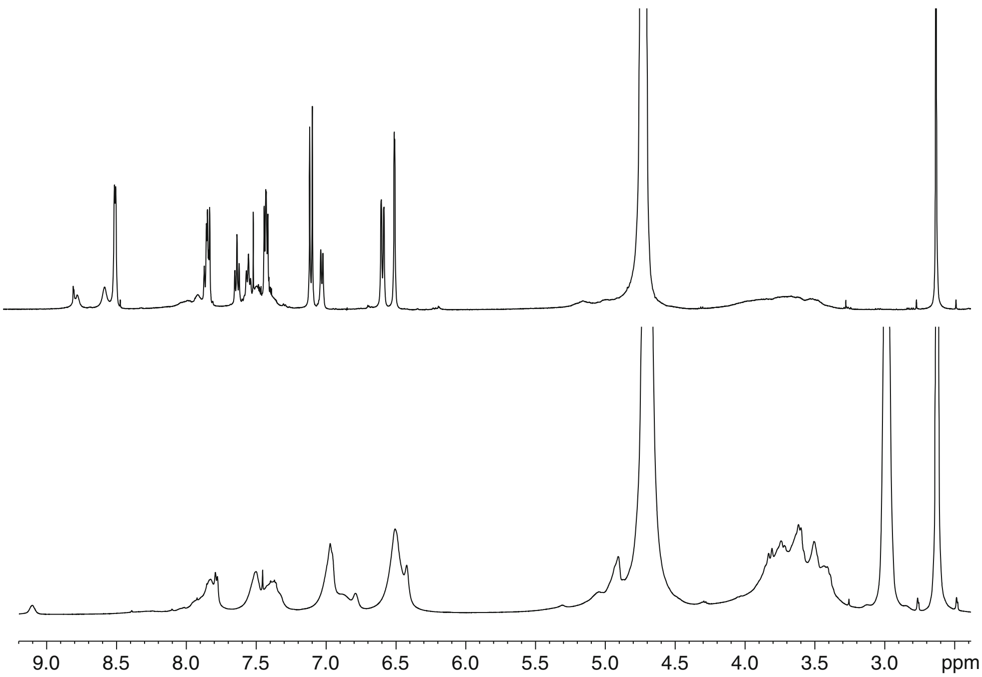

Fig. 5 HR MAS NMR spectra of CDNS12 (*bottom*) and CDNS14 (*top*) swollen with D_2O solution of fluorescein. Fluorescein spectrum lies in the region 6.5–9 ppm

Complementary information is provided by the analysis of diffusivity data of the solute. Table 1 indicate that the fluorescein self-diffusion coefficient, D (fluorescein), is dramatically different in CDNS12 and CDNS14, keeping constant the formal concentration of fluorescein in the CDNS. D (fluorescein) in CDNS12 equals that measured in a D_2O solution of the same concentration, whilst D (fluorescein) in CDNS14 is one order of magnitude higher, indicating an *acceleration effect with increasing mesh size of the cross-linked polymer*. This finding is totally counterintuitive. The rationale lies in the fact that the polar solute actually experiences, in its random motion, an electrostatic potential generated by the internal surface of the polymer network. The electrostatic component, along with the hydrodynamic one, contributes to diffusion in a non trivial manner. Comparable results were obtained by measuring the diffusivity of fluorescein entrapped in reference systems, agarose-carbomer hydrogels with known mesh size (ranging from 5 to 25 nm) and crosslinking density (ranging from 1 to 8 mmol/cm^3) [24]. Given the similarity of the polymer backbone of CDNS and agarose hydrogels (both carbohydrated based), and all the other factors (fluorescein concentration, temperature, etc.) being equal, similar values of diffusivity may be taken as semi-quantitative indication of mesh size and crosslinking density of the samples of CDNS. A theoretical model based on both electrostatic and hydrodynamic contribution to the diffusivity of a polar solute in a nanosized environment is being developed and will be detailed elsewhere [24]. At this stage, it suffices to stress that the experimental determination of diffusion coefficients of a model solute *within* the 3D network of CDNS represent a starting point for the rational design of applications, for example in the field of controlled release of pharmaceutically active components.

Conclusion

The use of three different methods of structural determination-Raman spectroscopy, X-ray diffraction and HR MAS NMR—allowed us to shed light on the structure of β cyclodextrin cross-linked polymers. Raman spectroscopy turned out to be a powerful method to monitor the cross-linking process via the low-frequency region. The hydration dynamics could also be investigated through the analysis of the vibration modes of O–H and C–H groups decoupled from the background of bulk water. Despite the fact that the CDNS of the present study are mainly amorphous, XRD gave information on the state of water in the swollen CDNS. HR MAS NMR allowed the measurement of diffusion coefficients of both water and dissolved solutes within the polymer network. Acceleration effects of the random motion of solute uncovered as a function of the CDNS mesh size (in turn related to the preparation) are a novel aspect of transport properties inside nanosized porous soft materials that gives opportunity for rational design of applications.

Acknowledgments Politecnico di Milano thanks Fondazione Cariplo (project 2007-5378) for financial support. This work was partially supported by the contribution from Provincia Autonoma di Trento (Italy).

References

1. Li, D., Ma, M.: New organic nanoporous polymers and their inclusion complexes. Chem. Mater. **11**, 872–874 (1999)
2. Trotta, F., Tumiatti, W.: Patent WO 03/085002 (2003)
3. Trotta, F., Tumiatti, W., Cavalli, R., Zerbinati, O., Roggero, C.M., Vallero, R.: Ultrasound-assisted synthesis of cyclodextrin-based nanosponges. Patent number WO 06/002814 (2006)
4. Trotta, F., Cavalli, R.: Characterization and applications of new hyper-cross-linked cyclodextrins. Compos. Interface. **16**, 39–48 (2009)
5. Cavalli, R., Trotta, F., Tumiatti, W.: Cyclodextrin-based nanosponges for drug delivery. J. Incl. Phenom. Macrocycl. Chem. **56**, 209–213 (2006)
6. Trotta, F., Tumiatti, W., Cavalli, R., Roggero, C. M., Mognetti, B., Berta, Nicolao, G.: Cyclodextrin-based nanosponges as a vehicle for antitumoral drugs. Patent WO 09/003656 (2009)
7. Vyas, A., Shailendra, S., Swarnlata, S.: Cyclodextrin based novel drug delivery systems. J. Incl. Phenom. Macrocycl. Chem. **62**, 23–42 (2008)
8. Swaminathan, S., Vavia, P.R., Trotta, F., Torne, S.: Formulation of beta-cyclodextrin based nanosponges of itraconazole. J. Incl. Phenom. Macrocycl. Chem. **57**, 89–94 (2007)
9. Mamba, B.B., Krause, R.W., Malefetse, T.J., Gericke, G., Sithole, S.P.: Cyclodextrin nanosponges in the removal of organic matter to produce water for power generation. Water SA. **34**, 657–660 (2008)
10. Mamba, B.B., Krause, R.W., Malefetse, T.J., Nxumalo, E.N.: Monofunctionalized cyclodextrin polymers for the removal of organic pollutants from water. Environ. Chem. Lett. **5**, 79–84 (2007)
11. Mhlanga, S.D., Mamba, B.B., Krause, R.W., Malefetse, T.J.: Removal of organic contaminants from water using nanosponge cyclodextrin polyurethanes. J. Chem. Technol. Biot. **82**, 382–388 (2007)
12. Arkas, M., Allabashi, R., Tsiourvas, D., Mattausch, E.-M., Perfler, R.: Organic/inorganic hybrid filters based on dendritic and cyclodextrin “nanosponges” for the removal of organic pollutants from water. Environ. Sci. Technol. **40**, 2771–2777 (2006)
13. Trotta, F., Tumiatti, W., Vallero, R.: Italian Patent No. MI2004 A000614
14. Huglin, M.B., Liu, Y., Velada, J.L.: Thermoreversible swelling behaviour of hydrogels based on *N*-isopropylacrylamide with acidic comonomers. Polymer **38**, 5791–5795 (1997)
15. Pilla, O., Caponi, S., Fontana, A., Goncalves, J.R., Montagna, M., Rossi, F., Viliani, G., Angelani, L., Ruocco, G., Monaco, G., Sette, F.: The low energy excess of vibrational states in v-SiO2: the role of transverse dynamics. J. Phys. Condense Matter **16**, 8519 (2004)
16. Fontana, A., Moser, E., Rossi, F., Campostrini, R., Carturan, G.: Structure and dynamics of hydrogenated silica xerogel by raman and brillouin scattering. J. Non-Cryst. Solids **212**, 292 (1997)
17. Sekine, Y., Ikeda-Fukazawa, T.: Structural changes of water in a hydrogel during dehydration. J. Chem. Phys. **130**, 034501 (2009)

18. Cruciani, O., Mannina, L., Sobolev, A.P., Segre, A., Luisi, P.: Multilamellar liposomes formed from phosphatidyl nucleosides: an NMR-HR MAS characterization. Langmuir **20**, 1144–1151 (2004)
19. Violette, A., Lancelot, N., Poschalko, A., Piotto, M., Briand, J.-P., Raya, J., Bianco, A., Guichard, G.: Exploring helical folding of oligoureas during chain elongation by high-resolution magic-angle-spinning (HRMAS) NMR spectroscopy. Chem. Eur. J. **14**, 3874–3882 (2008)
20. Mullen, M.K., Johnstone, K.D., Webb, M., Bampos, N., Sanders, J.K.M., Gunter, M.J.: Monitoring the thermodynamically controlled formation of diimide-based resin-attached rotaxanes by gel-phase HR MAS ^{1}H NMR spectroscopy. Org. Biomol. Chem. **6**, 278–286 (2008)
21. Schenetti, L., Mucci, A., Parenti, F., Cagnoli, R., Righi, V., Tosi, R.M., Tugnoli, V.: HR-MAS NMR spectroscopy of the human tissues: application to healthy gastric mucosa. Concept Magn. Reson A **28**, 430–443 (2006)
22. Holz, M., Heil, S.R., Sacco, A.: Temperature-dependent self-diffusion coefficients of water and six selected molecular liquids for calibration in accurate ^{1}H NMR PFG measurements. Phys. Chem. Chem. Phys. **2**, 4740–4742 (2000)
23. Raffaini, G., Ganazzoli, F.: Hydration and flexibility of α-, β-, γ- and δ-cyclodextrin: a molecular dynamics study. Chem. Phys. **333**, 128–134 (2007)
24. Perale, G., Rossi, F., Santoro, M., Marchetti, P., Mele, A., Castiglione, F., Raffa, E., Masi, M.: Drug release from hydrogels: a new understanding of transport phenomena (in press)